Your Interlibrary Loan request has been sent by email in a PDF format.

If this PDF arrives with an incorrect OCLC status, please contact lending located below.

Concerning Copyright Restrictions

FSU Faculty and Staff: Please refer to Copyright Resources Research Guide for additional information at http://guides.lib.fsu.edu/copyright

Interlibrary Loan Services: We Search the World for You…and Deliver!

Interlibrary Loan Services – FSU Community
Florida State University
R.M. Strozier Library
116 Honors Way
Tallahassee, Florida 32306-2047
Email: lib-borrowing@fsu.edu
Website: https://www.lib.fsu.edu/find-and-borrow/extended-borrowing
Phone: 850.644.4466

Non-FSU Institutions:
Email: lib-lending@fsu.edu
Phone: 850.644.4466

Cryogenics 141 (2024) 103901

Contents lists available at ScienceDirect

Cryogenics

journal homepage: www.elsevier.com/locate/cryogenics

Characterization of residual-resistance-ratio of Cu stabilizer in commercial REBCO tapes

Jun Lu [a,*], Yan Xin [a], Vince Toplosky [a], Jeremy Levitan [a], Ke Han [a], Jane Wadhams [a], Munir Humayun [a], Dmytro Abraimov [a], Hongyu Bai [a], Yifei Zhang [b]

[a] National High Magnetic Field Laboratory, Tallahassee, FL, USA
[b] SuperPower Inc., Glenville, NY, USA

ARTICLE INFO

Keywords:
Cu
Residual-resistance-ratio
Superconductor
REBCO

ABSTRACT

Residual-resistance-ratio (RRR) of Cu stabilizer in REBCO coated conductor is an important design parameter for REBCO magnets. Cu stabilizer with high RRR is especially beneficial for quench protections of REBCO magnets. In this work, we study RRR of electroplated Cu stabilizer in commercial REBCO tapes. We present RRR of over 180 samples measured for the quality assurance programs of REBCO magnet projects at the National High Magnetic Field Laboratory, USA (NHMFL). To investigate the factors that influence RRR, several samples were analyzed extensively by using scanning electron microscopy, secondary ion mass spectroscopy, and inductively coupled plasma mass spectroscopy. We found that RRR is strongly correlated with the grain size of Cu, which suggests that resistivity at low temperatures is dominated by grain boundary resistivity. In addition, low RRR corresponds to high concentration of chlorine impurity. This is explained by that higher chlorine impurity hindered the grain growth in the self-annealing process at room temperature which resulted in smaller grain size and low RRR. Annealing at 300C significantly enlarged the grain size and enhanced RRR. Due to the concern of critical current degradation, however, annealing is not recommended as a practical method to improve RRR of Cu in REBCO tapes.

1. Introduction

In a superconducting composite wire, a certain amount of stabilizer material with high electrical and thermal conductivity is necessary. Electrical conductivity of a metal at low temperatures is often assessed by residual-resistivity-ratio (RRR), defined as a ratio of resistivity at room temperature (295 K) and that at 4.2 K. The higher the RRR, the higher the electrical conductivity and the thermal conductivity at low temperatures. RRR of the stabilizer is a key design parameter for superconducting magnets.

High RRR Cu stabilizer in low temperature superconductor (LTS) wires is essential for stability of LTS magnets [1–6]. For REBCO magnets, thermal instability seems to be less of concern thanks to typically larger temperature margin. Nevertheless, RRR value of Cu stabilizer in REBCO tapes can still significantly influence magnet quench detection and protection. A high RRR is always desirable from the point of view of quench protection. The insert coils of the 32 T all-superconducting user magnet [7] developed at the National High Magnetic Field Laboratory, and the 40 T all-superconducting magnet currently under development [8] are made of 4 mm wide REBCO tapes with electroplated Cu stabilizer. Since high RRR of the Cu stabilizer of REBCO tapes is essential to ensure the performance of these magnets, we measured RRR as a part of the incoming material quality assurance program of the 32 T and the 40 T projects. Recently we found several samples that have RRR values significantly lower than the average. This motivated us to start an investigation on the factors influence RRR in the electroplated Cu with the goal of improving RRR.

It is well known that chemical impurities and microstructural defects can result in low RRR. In the case of electroplated Cu film, however, it is not clear which one of the two is mostly responsible and how to significantly improve its RRR. There are only few published research works on low temperature resistivity of electroplated copper films [9–11], and these studies were presented without chemical analyses. Therefore, in this paper we conducted a comprehensive experimental study on RRR of Cu stabilizer of commercial REBCO tapes. Several samples were analyzed in-depth using advanced material

* Corresponding author.
E-mail address: junlu@magnet.fsu.edu (J. Lu).

https://doi.org/10.1016/j.cryogenics.2024.103901
Received 10 May 2024; Accepted 17 July 2024
Available online 19 July 2024

characterization techniques. Inductively Coupled Plasma Mass Spectroscopy (ICP-MS) and Secondary Ion Mass Spectroscopy (SIMS) were performed to characterize the trace impurities in the Cu. Scanning electron microscopy (SEM) was used to investigate microstructure of these samples. We correlate the RRR values to chemical impurity and microstructure. The possibility of improving RRR of REBCO tapes is discussed.

2. Experimental method

The samples are 4 mm wide SCS4050-AP REBCO tapes made by SuperPower Inc. The REBCO conductors for the 32 T magnet project have 50 μm Cu stabilizer, and those for the 40 T magnet project have 20 μm Cu.

For RRR measurement, a 100 mm long sample was cut from each spool of conductor which was typically 100–200 m long. The surrounding Cu edges were trimmed by using a pair of scissors. Then the Cu/Ag stabilizer layer was peeled manually from the conductor as depicted in Fig. 1. The residual REBCO remained on the Ag layer was chemically removed by using a 0.6 % of nitric acid solution for about 3 min. The peeled 100 mm long film that contains the 20 or 50 μm Cu and about 2 μm Ag was used for resistance measurement. It is estimated that RRR is dominated by the Cu layer. The contribution of the Ag layer which has a measured RRR of about 15 is ignored.

Four-probe resistance measurements were performed at room temperature (295 K) and in liquid helium (4.2 K) in zero magnetic field. A pair of voltage taps typically 70 mm apart was soldered using $Pb_{37}Sn_{63}$ or $In_{49}Sn_{51}$ solders. Effort was made to reduce the size of solder spots to minimize the small positive error in the measured RRR due to superconductivity of $Pb_{37}Sn_{63}$ or $In_{49}Sn_{51}$ at 4.2 K. DC current of 1 A was delivered by a HP 6631B 10 V–8 A power supply. The voltage was measured by a Keithley 2010 digital multimeter.

Chemical trace element analyses were performed by Inductively Coupled Plasma Mass Spectrometry (ICP-MS). Cu/Ag film sample was dissolved by 14 N HNO_3 then acidified to form a 2 % HNO_3 solution that was directly analyzed. Elemental abundances were determined by ICP-MS using a Thermo Element XR™ equipped with an Elemental Scientific Inc. PFA spray chamber. The ICP-MS was tuned to yield >1 million counts/sec on 1 part per billion (ppb) tuning solution of ^{115}In. Peaks for 60 elements were monitored in low resolution mode. Concentrations in solution were converted into concentrations in the metal using gravimetrically determined sample weights.

Secondary Ion Mass Spectrometry (SIMS) was performed at Eurofins/EAG Laboratories to measure the depth profiles of O, Cl, P, S, and Fe in Cu. The depth profiling of Cu/Ag film began from the Ag layer with a 100 μm × 100 μm raster area. Cesium ion beam (Cs^+) was used for O, Cl, P, S analyses; and oxygen ion beam (O_2^+) was used for Fe analysis.

For microstructure analysis, Ga^+ ion beam imaging was performed using 24 pA current in a Thermal Scientific Helios G4 UC dual-beam field-emission SEM.

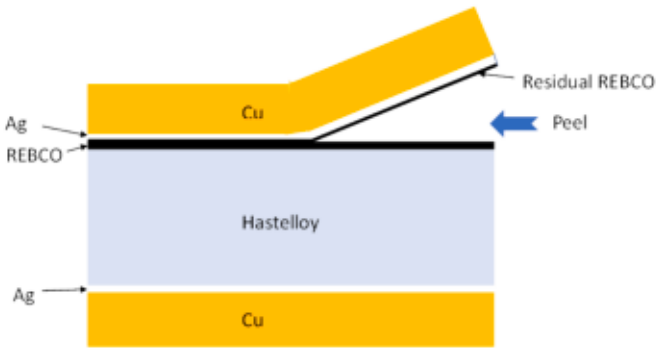

Fig. 1. A schematic of the layer structure of REBCO coated conductor where Cu/Ag layer above the REBCO layer is peeled off for RRR tests.

3. Experimental results

3.1. RRR of REBCO tapes for large magnet projects

RRR was measured as a part of incoming REBCO quality assurance for the 32 T and 40 T all-superconducting magnets projects at the National High Magnetic Field Laboratory, USA. For the 32 T project [7] which procured over 10 km of REBCO tapes from SuperPower, RRR of the 50 μm Cu stabilizer were tested for 89 out of total 250 piece-lengths. The results are plotted in Fig. 2(a). The average RRR of the total 89 samples is 57 with a standard deviation of 4. The maximum and minimum RRR are 68 and 50 respectively.

For the conceptual design phase of the 40 T project [8], a total of about 24 km of REBCO with 20 μm Cu stabilizer were procured from SuperPower. RRR were tested for 95 out of 155 piece-lengths. The results are plotted in Fig. 2(b). The average RRR is 47 with a standard deviation of 16. The maximum and minimum RRR are 85 and 19 respectively. Compared with Fig. 2(a), Fig. 2(b) showed large variation with several significantly low RRR cases. This lead to our detailed chemical and microstructural investigation of some Cu stabilizers. The results are shown in the following sections.

3.2. Chemical impurities in Cu stabilizer

Chemical impurities, especially oxygen, are usually the main cause of low RRR in bulk Cu. We measured impurity concentrations of two samples with RRR=25 and 60 respectively by ICP-MS. Valid data were obtained for more than 40 elements (not including O or Cl). No impurity was found above 1 ppm, except for Gd, Y and Ba which are evidently from the residuals of the REBCO layer.

SIMS depth profiles of O, P, S, Cl and Fe were performed on 3 samples with RRR=25, 37, and 60 respectively. Fig. 3(a) shows their O depth profiles. The depth profiling started from the side of the Ag layer. High level of O in depths 0–2 μm is due to the absorbed O in the Ag layer which is known to be permeable by oxygen. The O concentration quickly decreases and levels off in the Cu layer. The sample with the lowest RRR has the highest O concentration. In addition, Cl depth profiles in Fig. 3 (b) indicate that RRR values are strongly correlated with the Cl concentrations.

The measured impurities by ICP-MS and SIMS are summarized in Table 1 in ppm by weight. The data for O, Cl, and S are averages over depth of 6–10 μm from SIMS. Clearly O and Cl are the most prominent impurities. However, the measured O level cannot explain the relatively low RRR values. For example, 7.2 ppm of O would result in RRR=114 as estimated from Ref. [12], more than 4 times higher than the measured value of RRR=25. The direct effect of Cl on conductivity of Cu is not significant [13]. We will discuss the indirect impact of Cl later. Above chemical analyses suggest that O, Cl and other impurities are not directly responsible for the low RRR values.

3.3. Microstructures of Cu stabilizer

A significant contribution to resistivity comes from the electron scattering by structural defects, as represented by the term ρ_{defect} in equation (1). Resistivity at grain boundaries, in particular, is very important [14–18]. The smaller the grain size, the more the grain boundaries, the higher the resistivity, the lower the RRR. We examined the microstructures of samples of different RRR by SEM. Fig. 4(a)–(c) are cross-sectional ion beam images of Cu stabilizer with RRR=25, 48, and 87 respectively. Apparently, samples with smaller grain size have lower RRR. The twin boundaries can be distinguished from grain boundaries by its straightness. It should be noted that Fig. 4(a) and (b) were taken from the Cu on the opposite side of the REBCO layer (the backside). With the identical electroplating conditions, the microstructure of the Cu film

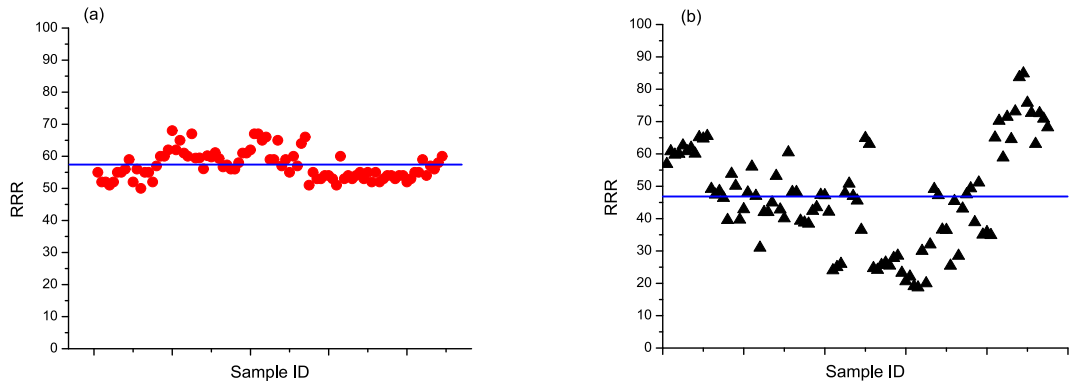

Fig. 2. Measured RRR of Cu stabilizer of REBCO for (a) 32 T magnet project conductors with 50 m Cu (total 89 data), (b) 40 T magnet project conductors with 20 m Cu (total 95 data). The solid horizontal lines represent the average RRR values.

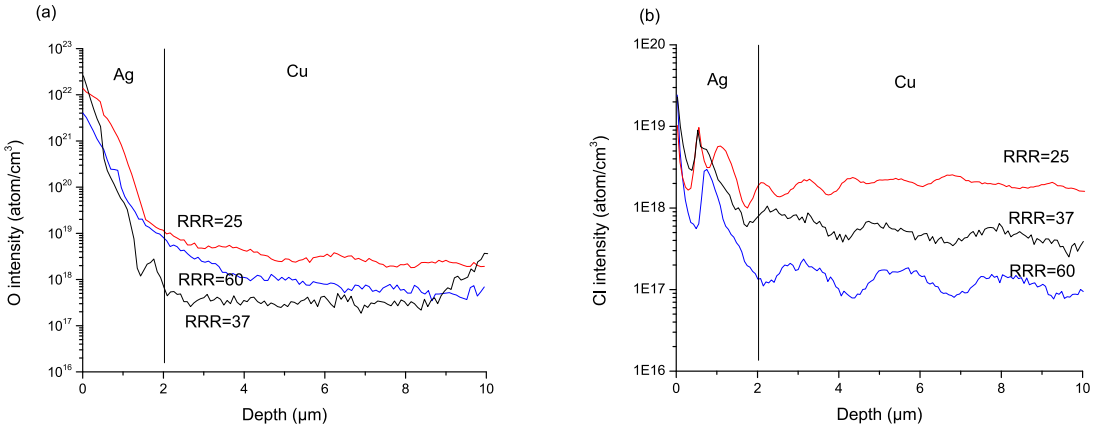

Fig. 3. SIMS depth profiles of (a) O in Cu stabilizer of different RRR, (b) Cl in Cu stabilizer of different RRR. The profiling started from the Ag layer. The initial 2 m is the Ag layer which is known to permeable to O.

Table 1
Impurity concentrations in Cu stabilizers.

Element	Concentration (ppm in weight)		
	RRR 25	RRR 37	RRR 60
O	7.2	1.8	2.7
Cl	14.2	3.1	0.9
S	0.1	DL	DL
P and Fe	DL	DL	DL
Other elements	1.0		1.0

* DL is the detection limits. 0.5 ppm for Fe; 0.03 ppm for S; 0.06 ppm for P.

of both sides should be identical. The average grain sizes were analyzed from Fig. 4 by counting number of intersections between grain boundaries and horizontal lines that are at different distances from the Cu/Ag interface. In these analyses, we ignored twin boundaries, because twin boundaries have at least one order of magnitude lower resistivity than grain boundaries [16]. Table 2 lists the grain sizes measurement results, which indicates that RRR values are strongly correlated with the grain size, suggests that grain boundaries are mostly responsible for the resistivity in these samples. Another observation made from Fig. 4 is that grain size is significantly smaller near the Cu/Ag interface where the electroplating process started. The grain size gradually increased as the Cu grew thicker. This could partially be the reason why the average RRR for the 32 T magnet conductors is slightly higher than that for the 40 T magnet conductors.

3.4. *Effect of annealing*

It is well known that annealing of Cu enlarges the grain size. So an experiment was designed to verify that the increase in RRR is correlated with the increase of grain size by annealing, which would support that RRR in our samples was dominated by grain boundary resistivity. Table 3 lists RRR values of several samples before and after annealing of REBCO samples at 300C for 30 min in argon. As expected, RRR increased considerably by the annealing for all the samples. Meanwhile the grain size was also significantly increased as shown by SEM images in Fig. 5 (for sample D in Table 3). This correlation of RRR increment and grain growth was confirmed.

Furthermore, it is of practical interest to explore the possibility of improving Cu RRR by annealing the as received REBCO tapes. It is known that annealing at temperatures higher than 200C causes significant degradation in critical current of REBCO tapes [19]. Therefore, we annealed a low RRR (RRR 25) sample at temperatures of 80 140C for 2 h. Annealing at these temperatures, as shown in Fig. 6, did not improve RRR much. Significant improvements were observed only at temperatures above 200C (for 0.5 h.) where degradation of critical current would be a concern. Therefore, annealing as received REBCO tape does not seem to be suitable method to improve RRR of REBCO without suffering a loss in critical current.

4. Discussions

4.1. *Effect of magnetoresistivity*

RRR of Cu presented above is measured in zero magnetic field. In

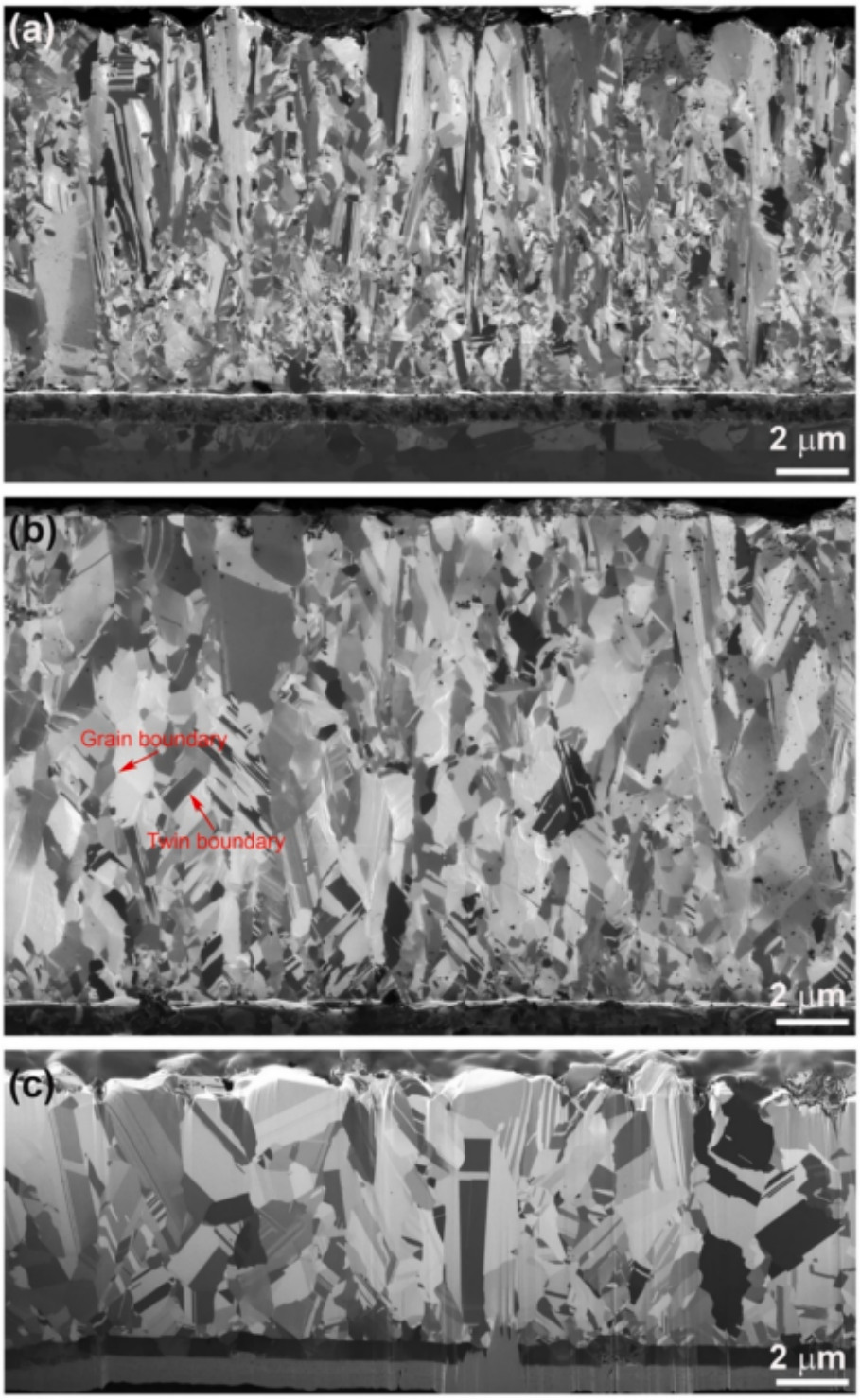

Fig. 4. SEM ion beam images of Cu stabilizers (a) RRR=25 (b) RRR=48, (c) RRR=87.

Table 2
Cu grain size measured from Fig. 4.

Distance from Cu/Ag interface (μm)	Grain size (μm)		
	RRR=25	RRR=48	RRR=87
5	1.3	1.9	2.5
10	1.4	2.0	2.7
15	2.0	2.0	3.6
Average	1.5	2.0	2.8

Table 3
Effect of annealing at 300C for 30 min in argon.

Sample	RRR before	RRR after
A	48	73
B	23	65
C	24	85
D	25	76

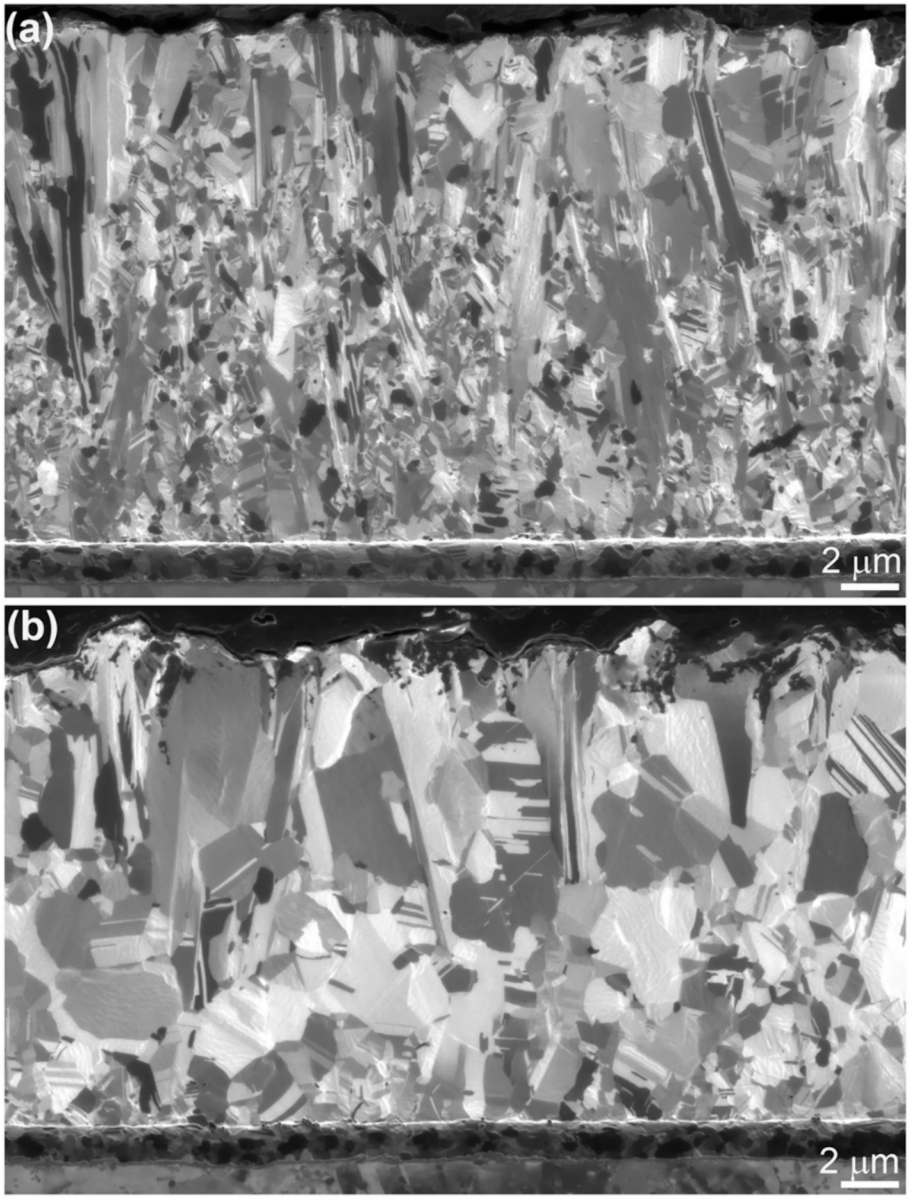

Fig. 5. SEM ion beam images of a sample of RRR 25 before (a) and after (b) annealing at 300C for 30 min. After annealing RRR was measured to be 76 (sample D in Table 3).

high magnetic fields, the magnetoresistivity of copper is significant. The effect of magnetoresistivity on RRR is discussed here. According to Matthiessen s rule, resistivity of a pure metal may be written in the form,

$$\rho \quad \rho_{thermal} \quad \rho_{impurity} \quad \rho_{defect} \quad \rho_{magneto} \tag{1}$$

where $\rho_{thermal}$ is the resistivity due to thermal vibration of the lattice which leads to electron phonon scattering. $\rho_{impurity}$ is due to the scattering by impurity atoms; and ρ_{defect} is due to the scattering by structural defects such as dislocations and grain boundaries. The last term $\rho_{magneto}$ is the contribution from magnetoresistivity.

The term $\rho_{thermal}$ can be formulated by a Block-Gruneisen function and is dominant at room temperature even in high magnet fields. At temperatures below 20 K, however, $\rho_{thermal}$ is negligibly small. At these temperatures in zero field, $\rho_{impurity}$ and ρ_{defect} are more important terms. Therefore, to reduce the zero field resistivity at low temperatures, one needs to minimize the chemical impurities and structural defects. In high magnetic fields, magnetoresistivity becomes appreciable. Magnetoresistance in copper is originated from its non-spherical Fermi surface and it follows Kohler s rule, which can also be derived theoretically from Boltzmann transport equations [20].

$$\rho_{magneto} \ \rho \ 0 \quad \text{function } B \ \rho \ 0 \tag{2}$$

where B is the magnetic field, $\rho(0)$ is the resistivity in zero field. When magnetic field is perpendicular to the electric current (transverse field), which is the case for most magnet applications, the magnetoresistivity $_{\text{magneto}}$ in Cu at temperature T can be calculated by an empirical formula [12],

$$\text{Log}(\ _{magneto}/\ _{0}(T)) \quad -2.662 \quad 0.3168 \log(B\ S(T)) \quad 0.6229 (\log(B\ S(T))^2 \quad 0.1839 (\log(B\ S(T))^3 \quad 0.01827(\log(B\ S(T))^4 \tag{3}$$

where ρ_0 (T) is the zero-field resistivity at temperature T in -m, B is the magnetic field in tesla, $S(T)$ $\rho_0(273\ \text{K})/\ \rho_0(T)$. Equation (2) and (3) show that magnetoresistivity of Cu increases with field and decreases zero field resistivity. It is used to calculate $\rho_{magneto}(B, 4.2\ \text{K})$ for different $\rho_0(4.2\ \text{K})$. We define an effective RRR in magnetic field, RRR_{eff} as

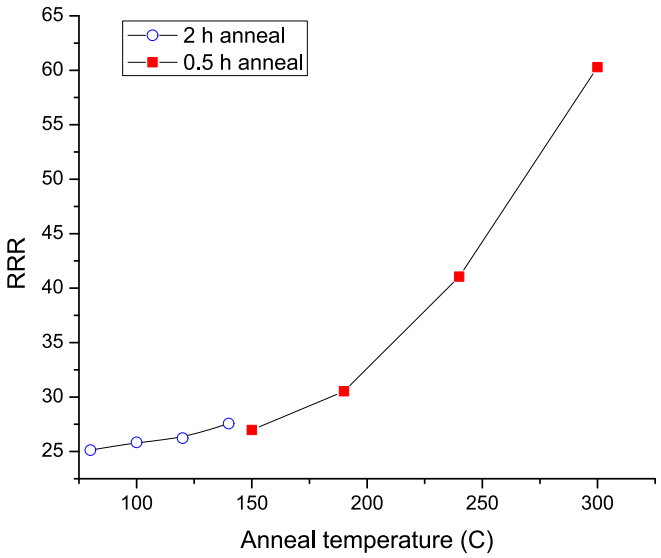

Fig. 6. RRR vs. annealing temperature.

$$RRR_{eff} \quad \rho_0 \ 295K \quad r_0 \ 4\ 2K \quad r_{magneto} \ B \ 4\ 2K \tag{4}$$

We calculated RRR_{eff} using Eqs. (3) and (4). Fig. 7 plots the calculated RRR_{eff} as a function of magnetic field for different RRR values. For high RRR materials, RRR_{eff} decreases quickly with magnetic field B. For instance, for RRR 150, the RRR_{eff} is lowered to less than 30 in a 12 T field. At higher fields as shown in the inset, the magnetoresistivity makes such a prominent contribution that the RRR_{eff} is lower than 20 for all RRR values. The benefit of high conductivity Cu in zero-field is much compromised in high fields. It is important to note, however, even at high fields, very low RRR still has significant negative impact to the RRR_{eff}. For example, at 40 T, RRR_{eff} of RRR 50 is still 70 % higher than that of RRR 10. Therefore, it can be concluded that in spite of the significant magnetoresistivity effect, Cu stabilizer with RRR 50 is still very desirable for high field magnets.

4.2. *Effect of Cu microstructure*

Cu resistivity increases with microstructural defects which include dislocations, grain boundaries and other defects as shown in Eq. (1). For instance, Cu resistivity increases significantly with cold work which introduce microstructural defects [12]. The effect of grain boundaries on Cu resistivity is well established [14 18]. The grain boundary resistivity ρ_G can be related to the grain size d by a simple relationship [14],

$$\rho_G \quad A \ d \tag{5}$$

where A 7.22 10 ^{16} -m^2 is a constant obtained from fitting experimental data [16]. If ρ_G dominates the resistivity at 4.2 K in zero field, Eq. (4) can be rewritten in term of RRR as,

$$RRR \quad \rho_{295K} \ \rho_G \quad \rho_{295K} \ A \ d \quad K \ d \tag{6}$$

where ρ_{295K} 1.72 x 10^{-8} m is the resistivity of annealed copper at 295 K, so ρ_{295K}/A K 23.8 m ^{1}. In such case, RRR is proportional to the grain size, and a grain size of 1 m corresponds to a RRR of 23.8. In Fig. 8, we plot the measured RRR versus the grain size obtained from Table 3. The estimated measurement uncertainty in grain size is 0.5 m. The solid line is calculated by equation (5) for comparison. Considering the appreciable uncertainties in grain size measurement of this work as well as Ref. [16] where parameter A of equation (5) was obtained, the agreement between the experimental data and the prediction by equation (5) is satisfactory. This is consistent with the correlation between RRR and grain size in Ref. [11]. The results in Fig. 8 suggest that resistivity from chemical impurities is not significant. Grain boundary resistivity is the dominant mechanism responsible for the observed low RRR.

It is well known that electroplated Cu film undergoes a self-annealing within a few tens of hours of deposition [21 23]. In the self-annealing process, the grain size grows at room temperature, and resistivity decreases by up to 20 % [22]. It means that before self-annealing 20 % of the resistivity is from grain boundaries which alone renders a RRR of only 5. Compared with RRR after self-annealing of about 50 as shown in Fig. 2(a) and (b), such a dramatic RRR enhancement highlights the importance of the self-annealing process. Any mechanism that hinders the self-annealing process would inevitably cause low RRR as will be discussed in the next section. After self-annealing, further increment of RRR becomes negligibly small. For instance, we measured a sample with RRR of 25 six months after the initial measurement, RRR remained the same.

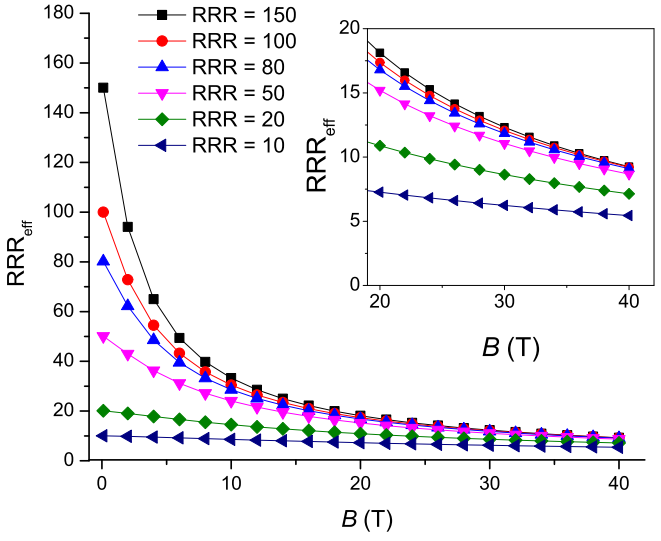

Fig. 7. The effect of magnetic field on RRR_{fm} as calculated by equations (2) and (3). RRR_{mf} is plotted as a function of magnetic field for different RRR. The inset is a close-up for magnetic fields above 20 T.

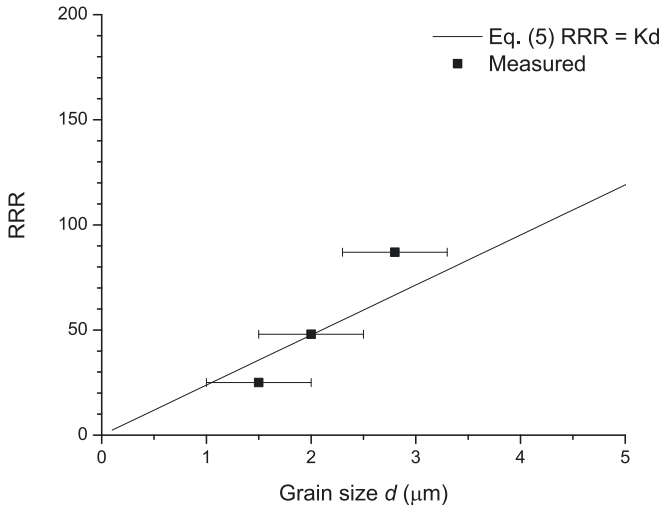

Fig. 8. RRR versus Cu grain size compared with the calculated relationship of equation (5). The estimated uncertainty in the measured gain size is 0.5 m. The solid line is the prediction by equation (5).

4.3. Impurity in electroplated Cu

Chemical impurity, especially oxygen, is usually the biggest contributor to residual resistivity in bulk Cu. During the electroplating process, however, the Cu film (cathode) has an accumulation of reduced hydrogen which inhibits high level of oxygen from forming in the electroplated film. This explains the relatively low oxygen content in our samples measured by SIMS. To make Cu films smooth and bright, sometimes additives, which often contains S, P, and Cl, are added in the plating bath [24]. In such case, S, P, and Cl are often detected in Cu, which can result in low RRR. Since there were no additives in the plating bath for the SuperPower conductors, the concentrations of S and P were negligibly low. Cl concentration, however, was surprisingly high especially in low RRR samples, even though no Cl was intentionally added in the bath. Moreover, it is unexpected that Cl concentration is strongly correlated with RRR (Fig. 3(b)), because Cu resistivity has not been reported to be sensitive to Cl concentration, and we proved that microstructural defects are mostly responsible for RRR of our samples. Interestingly, it was previously reported that high concentration of Cl in electroplated Cu hinders the grain growth in the self-annealing process [25]. This is consistent with our observation that samples with higher Cl have smaller grain sizes. Therefore, we conclude that high concentration of Cl deterred grain growth during self-annealing. This resulted in small grain size in high Cl samples. The small grain size in-turn resulted in low RRR, since grain boundary resistivity is mostly responsible for RRR. This explains why high Cl samples exhibit low RRR.

5. Conclusions

The RRR of Cu stabilizers of over 180 REBCO samples were measured. Their typical RRR value was about 50. Electron microscopy revealed that Cu grain size increased with increasing RRR, which is consistent with the relationship between Cu resistivity and grain size in the literature. This proved that grain boundary resistivity is mostly responsible for the RRR in our samples. Annealing at elevated temperatures resulted in grain growth. As a result, RRR of samples annealed at 300C is considerably higher. Due to the issue of critical current degradation, however, annealing is not recommended for improving RRR. Chemical impurities O, Cl, S, P, Fe and other elements in Cu were measured by SIMS and ICP-MS. Cl concentration was strongly correlated with RRR. This is explained by that relatively high concentration of Cl deterring Cu grain growth during the self-annealing at room temperature, and the smaller grain size resulted in lower RRR.

CRediT authorship contribution statement

Jun Lu: Data curation, Formal analysis, Funding acquisition, Investigation, Methodology, Project administration, Resources, Supervision, Validation, Visualization, Writing original draft, Writing review & editing. **Yan Xin:** Conceptualization, Data curation, Formal analysis, Investigation, Methodology, Resources, Visualization. **Vince Toplosky:** Data curation. **Jeremy Levitan:** Data curation. **Ke Han:** Formal analysis, Investigation. **Jane Wadhams:** Data curation. **Munir Humayun:** Data curation, Investigation, Methodology. **Dmytro Abraimov:** Investigation, Methodology. **Hongyu Bai:** Conceptualization, Investigation, Project administration, Resources. **Yifei Zhang:** Funding acquisition, Investigation, Methodology, Resources, Validation.

Declaration of competing interest

The authors declare that they have no known competing financial interests or personal relationships that could have appeared to influence the work reported in this paper.

Data availability

Data will be made available on request.

Acknowledgement

Dr. Hang Dong Lee and Dr. Steven Liu of Eurofins / EAG Laboratories are acknowledged for their contribution in SIMS analyses. This work was performed at the National High Magnetic Field Laboratory, which is supported by National Science Foundation Cooperative Agreement No. DMR-1644779, DMR-1839796, DMR- 2131790, and the State of Florida.

References

[1] Dietderich DR, et al. Correlation between strand stability and magnet performance. IEEE Trans Appl Supercond 2005;15(2):1524.
[2] Bordini B, et al. Impact of the residual resistivity ratio on the stability of Nb3Sn magnets. IEEE Trans Appl Supercond 2012;22(3):4705804.
[3] Ghosh AK. Effect of copper resistivity and filament size on the self-field instability of high-Jc Nb3Sn strands. IEEE Trans Appl Supercond 2013;23(3):7100407.
[4] Charifoulline Z. Residual Resistivity Ratio (RRR) measurements of LHC superconducting NbTi cable strands. IEEE Trans Appl Supercond 2006;16(2):1188.
[5] Lu J, et al. Comparative measurements of ITER Nb3Sn strands between two laboratories. IEEE Trans Appl Supercond 2017;27(5):6001004.
[6] Levitan J, et al. Verification testing of MQXFA Nb3Sn wires procured under LARP. IEEE Trans Appl Supercond 2019;29(5):6000904.
[7] Markiewicz WD, et al. Design of a superconducting 32 T magnet with REBCO high field coils. IEEE trans Appl Supercond 2012;22(3):4300704.
[8] Bai H, et al. The 40 T superconducting magnet project at the national high magnetic field laboratory. IEEE Trans Appl Supercond 2020;30(4):4300405.
[9] Bonura M, Senatore C. High-field thermal transport properties of REBCO coated conductors. Supercond Sci Technol 2015;28:025001.
[10] Fouaidy M, Hammoudi N. RRR of copper coating and low temperature electrical resistivity of material for TTF couplers. Physica C 2006;441:137.
[11] Okii Y, et al. R&D of copper electroplating process for power couplers: effect of microstructures on RRR. In: 19th Int conf on RF superconductivity, Dresden, Germany; 2019. p. 278. doi:10.18429/JACoW-SRF2019-MOP083.
[12] Simon NJ, Drexler ES, Reed RP. Properties of copper and copper alloys at cryogenic temperatures. U.S. Government printing office, Washington 1992.
[13] Lee W-H, et al. Effect of halides on Cu electrodeposit film: potential-dependent impurity incorporation. J Electrochem Soc 2017;164(7):D493.
[14] Andrews PV. Resistivity due to grain boundaries in pure copper. Phys Lett 1959;19:558.
[15] Nakamichi I. Electrical resistivity and grain boundaries in metals. Mater Sci Forum 1996;207 209:47.
[16] Bakonyi I. Accounting for the resistivity contribution of grain boundaries in metals: critical analysis of reported experimental and theoretical data for Ni and Cu. Eur Phys J Plus 2021; 136: 410. https://doi.org/10.1140/epjp/s13360-021-01303-4 .
[17] Bishara H, et al. Understanding grain boundary electrical resistivity in Cu: the effect of boundary structure. ACS Nano 2021;15:16607. https://pubs.acs.org/action/showCitFormats?doi 10.1021/acsnano.1c06367&ref pdf.
[18] Sun T, Yao B, Warren AP, Barmak K, Toney MF, Peale RE, et al. Surface and grain-boundary scattering in nanometric Cu films. Phys Rev B 2010;81:155454.
[19] Lu J, et al. Oxygen out-diffusion in REBCO coated conductor due to heating. Supercond Sci Technol 2021;34:075004.
[20] Rosenberg HR. Low temperature sold state physics. London: Oxford at the Clarendon Press; 1963. p. 108.
[21] Wendrock H, et al. Room temperature grain growth in electroplated copper. Microelectron Reliab 2000;40:1301.
[22] Stangl M, et al. Characterization of electroplated copper self-annealing with investigations focused on incorporated impurities. Microelectron Eng 2005;82:189.
[23] Chen C-C, et al. Depth-dependent self-annealing behavior of electroplated Cu. Surf Coat Technol 2017;320:489.
[24] Lee H, Chen C-M. Impurity effects in electroplated-copper solder joints. Metals 2018;8:388. https://doi.org/10.3390/met8060388.
[25] Huang Q, et al. Effects of impurity elements on isothermal grain growth of electroplated copper. J Electrochem Soc 2018;165(7):D251.